



Synthesis, fluorescence properties, and conformational analysis of ether-linked (1,8)pyrenophanes

Hajime Maeda ^{a,*}, Makoto Geshi ^a, Kenji Hirose ^a, Taniyuki Furuyama ^{a,b}, Masahito Segi ^a

^a Division of Material Chemistry, Graduate School of Natural Science and Technology, Kanazawa University, Kakuma-machi, Kanazawa, Ishikawa 920-1192, Japan

^b Japan Science and Technology Agency (JST)-PRESTO, 4-1-8 Honcho, Kawaguchi, Saitama 332-0012, Japan

ARTICLE INFO

Article history:

Received 17 June 2019

Received in revised form

31 July 2019

Accepted 6 August 2019

Available online xxx

Keywords:

Cyclophane

Pyrene

Pyrenophane

Fluorescence

Excimer

ABSTRACT

Mono-, di- and oligo-ether linked (1,8)pyrenophanes **1–7** were synthesized, and their fluorescence and conformational properties in the absence and presence of metal ions were elucidated. Fluorescence spectra of 1.0×10^{-5} M solutions of the mono- and di-ether linked pyrenophanes **1–5** were comprised of only monomer emission bands, while those of the oligoethylene glycol linked analogs **6** and **7** contained both monomer and intramolecular excimer emission bands. Addition of perchlorate salts of Ba^{2+} , Na^+ and Li^+ to 1:1 v/v $\text{CH}_3\text{CN}:\text{CH}_2\text{Cl}_2$ solutions of **6** and **7** caused decreases in the intensities of the corresponding intramolecular excimer emission bands and, in some cases, increases in the intensities of the monomer emission. Monomer and intramolecular excimer emission from the (1,8)pyrenophanes are suggested to arise from the respective *anti* and *syn* conformers, whose ratios are dependent on solvent polarity, temperature and kinds of added metal ions.

© 2019 Elsevier Ltd. All rights reserved.

1. Introduction

Since pyrene has a dual fluorescence character (monomer and excimer), a high fluorescence quantum yield and photostability, it is often used as a fluorescence reporter group [1–14]. Pyrenophanes that contain linked two pyrene moieties have attracted much attention in view of their characteristic fluorescence properties (monomer and intramolecular excimer), structures (plain or bent), and molecular recognition abilities (guest inclusion) (Scheme 1) [5,15]. (2,7)Pyrenophanes have the highest symmetry and, as a result, are not capable of existing as conformational isomers [16–25]. In contrast, the pyrene moieties in (1,6)pyrenophanes can exist in two different orientations that correspond atropisomers having C_{2h} and D_2 symmetries [21,23,26–31]. In addition, *syn* and *anti* conformers are possible for (1,3)pyrenophanes [32–35]. We have previously demonstrated that equilibrium populations of *syn* and *anti* conformers of oxygen-, sulfur- and selenium-linked [3.3](1,3)pyrenophanes are influenced by solvent polarity and temperature, and that these populations govern their fluorescence characteristics [36,37]. Like (1,3)pyrenophanes, (1,8)pyrenophanes also have the capability of existing as *syn* and *anti* conformers.

However, in contrast to other pyrenophanes, which have been subjected to extensive studies, descriptions of the synthesis of (1,8)pyrenophanes is limited [26] and studies have not been conducted to assess the equilibrium between their *syn* and *anti* conformational isomers.

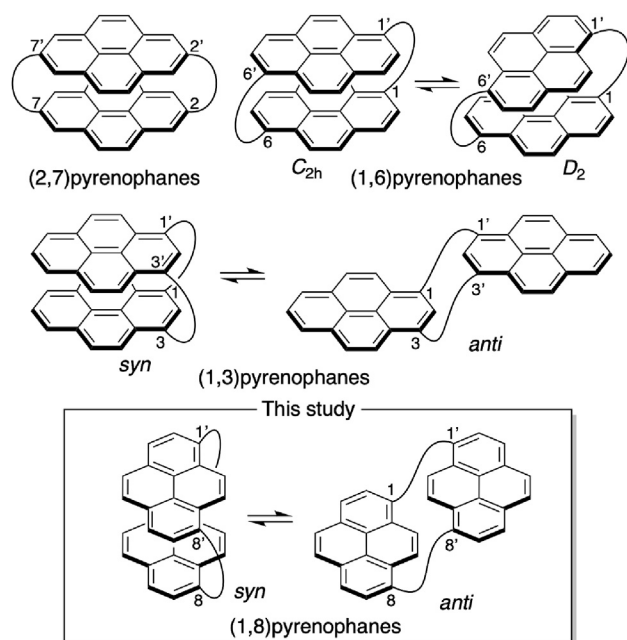
The investigation described below focused on the development of novel fluorescence switching molecules. For this purpose, mono-, di- and oligo-ether linked (1,8)pyrenophanes **1–7** were synthesized, and their fluorescence properties and conformational preferences were assessed.

2. Results and discussion

The pathways employed for the synthesis of (1,8)pyrenophanes **1–7**, shown in Scheme 2, began with oxidation of pyrene (**8**) to form pyrene-4,5-dione (**9**) [38,39], which was bis-methylated to produce 4,5-dimethoxypyrene (**10**). Dibromination of **10** at the 1,8-position [40,41] followed by formylation and reduction produced diol **13**, which upon bromination and iodination formed the respective dibromide **14** and diiodide **15**. Pyrenophane **1** was then generated by reaction of **13** with **14** in the presence of NaH in 7% yield. Pyrenophanes **2–7**, which possess di- and oligo-ether linkages, were prepared in 6–18% yields by reactions of **14** or **15** with various diols. The low yields are a consequence of formation of larger cyclic

* Corresponding author.

E-mail address: maeda-h@se.kanazawa-u.ac.jp (H. Maeda).

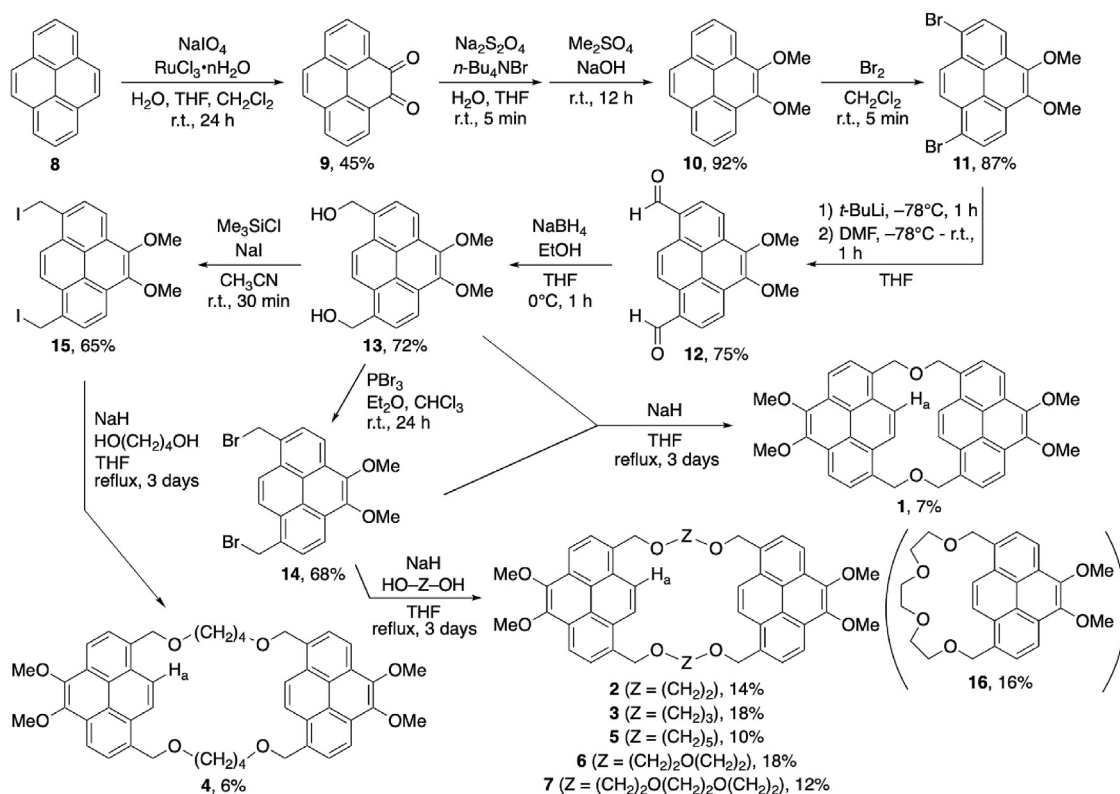


Scheme 1. Conformers of pyrenophanes.

oligomers that were not isolated and characterized. In the reaction producing **7**, the pyrenocrown ether **16** was also formed in 16% yield [42].

UV–vis absorption spectra of 1.0×10^{-5} M DMF, CH_2Cl_2 , CHCl_3 , THF and toluene solutions of pyrenophanes **1–7** contained broad bands in the region of 320–380 nm arising from $\pi-\pi^*$ transitions of

the pyrene chromophore (Fig. S1). Fluorescence spectra of these solutions differed greatly depending on the nature of the pyrenophane linking chains (Fig. 1). Although the fluorescence bands of **1** occurred at relatively longer wavelength than do those that arise from monomer emission of common pyrene derivatives [10,11], they are attributed to monomer emissions because of their short fluorescence lifetimes (2.05 ns in CH_2Cl_2 , 1.02 ns in THF) (Fig. S2). Pyrenophanes **2–5** fluoresced with emission maxima at ca. 400 nm. Because of their wavelength maxima and shapes, these bands are also associated with monomer emission. The fluorescence of **3** is slightly different from **2**, **4**, and **5** probably because the difference in structure or motion of the molecule is involved. The preference for monomer fluorescence displayed by mono- and di-ether linked pyrenophanes **1–5** markedly differs from that of 1,ω-dipyrenylalkanes $\text{Py}(\text{CH}_2)_n\text{Py}$ ($n=3-5$), which display intense intramolecular excimer emission [3]. These phenomena are likely a consequence of ring strain present in **1–5** that prevents formation of *syn* conformers in which $\pi-\pi$ stacking interactions exist between the pyrene rings. In addition, the fluorescence bands of **1–5** shifted to longer wavelengths and their intensities decreased with increasing solvent polarity. This phenomenon is often observed for monomer emission from methoxy-substituted pyrenes [43,44], owing to the stabilization effect of more polarized excited states by more polar solvents. In contrast, both monomer and intramolecular excimer emission bands existed in fluorescence spectra of **6** and **7**. Moreover, the ratios of the intensities of intramolecular excimer to monomer emission ($I_{\text{ex}}/I_{\text{mon}}$) of **6** and **7** increased with increasing solvent polarity, seen quantitatively in the plot of $I_{\text{ex}}/I_{\text{mon}}$ versus $E_{\text{T}}(30)$ [45] given in Fig. 2. Both **5** and **6** have 9 atoms in chains linking their pyrene rings, however, their fluorescence properties were significantly different. This might be a consequence of the fact that the methylene chains in **5** should favor the all-*anti* conformation while the all-*gauche* conformation should be favored in the

Scheme 2. Synthesis of (1,8)pyrenophanes **1–7**.

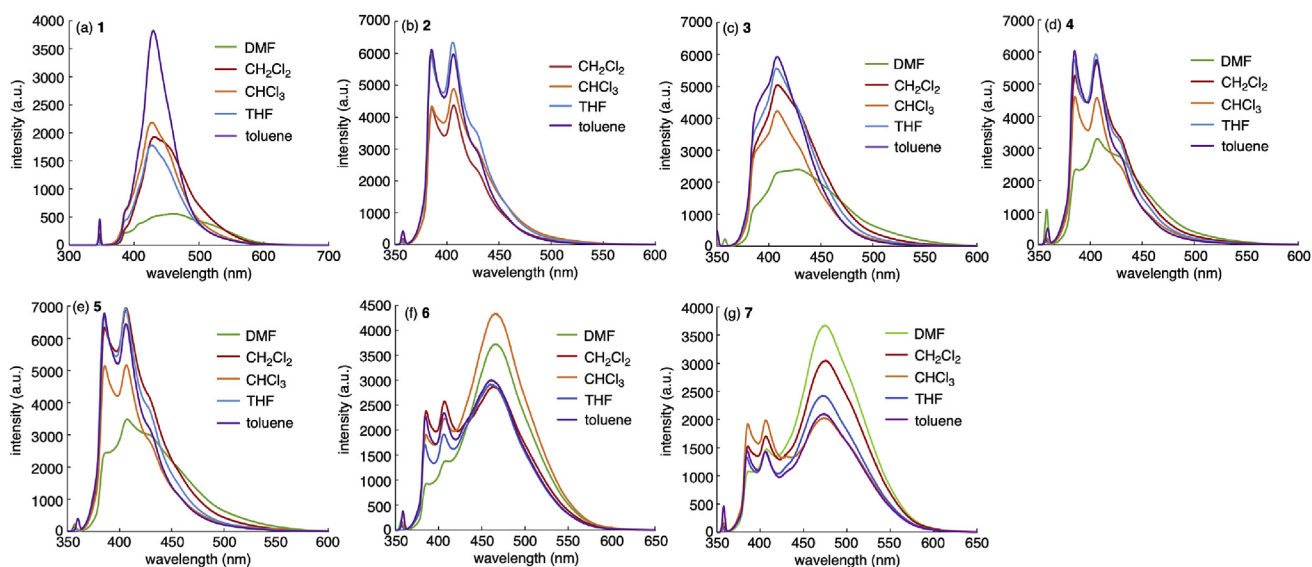


Fig. 1. Fluorescence spectra (1.0×10^{-5} M) of (a) **1**, $\lambda_{\text{ex}} = 345\text{--}347$ nm, (b) **2**, $\lambda_{\text{ex}} = 357\text{--}358$ nm, (c) **3**, $\lambda_{\text{ex}} = 348\text{--}358$ nm, (d) **4**, $\lambda_{\text{ex}} = 357\text{--}359$ nm, (e) **5**, $\lambda_{\text{ex}} = 357\text{--}360$ nm, (f) **6**, $\lambda_{\text{ex}} = 357\text{--}359$ nm, and (g) **7**, $\lambda_{\text{ex}} = 357\text{--}359$ nm, r.t.

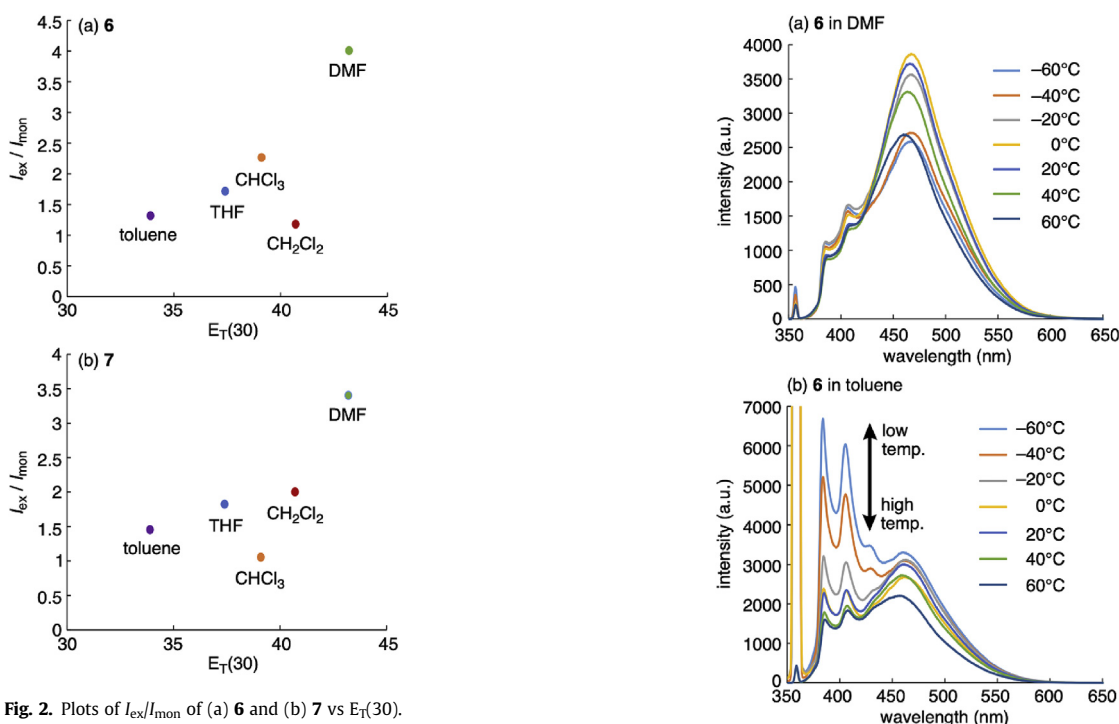


Fig. 2. Plots of $I_{\text{ex}}/I_{\text{mon}}$ of (a) **6** and (b) **7** vs $E_T(30)$.

corresponding oligoethylene glycol chains in **6** [46,47].

Information about relationships between preferred conformations of the pyrenophanes and their emission properties has come from variable-temperature fluorescence studies of **1–7** in DMF and toluene (Figs. S3 and S4). Inspection of the fluorescence spectra of **1–5** in both DMF and toluene showed that the intensities of the monomer emission bands increased with decreasing temperature. Importantly, different behavior was observed for **6** (Fig. 3) where emission from an intramolecular excimer occurred in DMF regardless of temperature, whereas in toluene the ratio of monomer to excimer emission intensities increased with decreasing temperature. A similar temperature dependence of emission was observed in variable temperature fluorescence studies with **7**

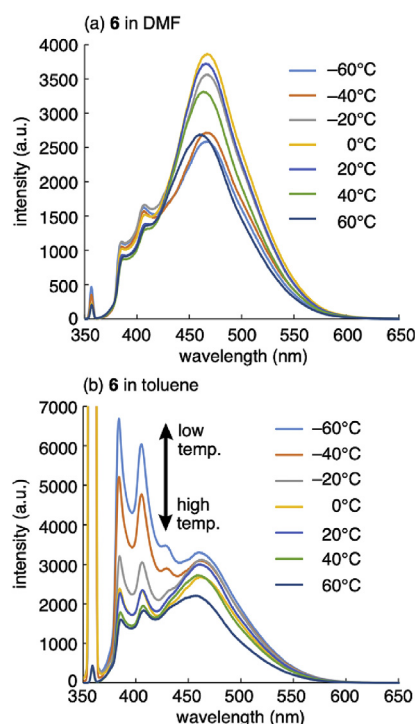


Fig. 3. Variable-temperature fluorescence spectra (1.0×10^{-5} M) of **6** in (a) DMF, $\lambda_{\text{ex}} = 356$ nm, and (b) toluene, $\lambda_{\text{ex}} = 359$ nm.

(Fig. S3k,l).

Variable-temperature ^1H NMR spectroscopic studies were carried out with **1–7** in DMF- d_7 and toluene- d_8 (Fig. S5). A remarkable temperature effect on any proton resonance was not observed in the cases of **1–5**. In contrast, the resonance for the inner protons in **6** (Fig. 4), marked as H_a in the structure displayed in Scheme 2, appeared at 8.53 ppm at 40 °C in DMF- d_7 and did not change as the temperature was lowered to -60 °C. In contrast, the resonance for H_a in the spectrum of **6** in toluene- d_8 shifted downfield from 8.52 (60 °C) to 9.21 ppm (-80 °C) as the temperature was lowered.

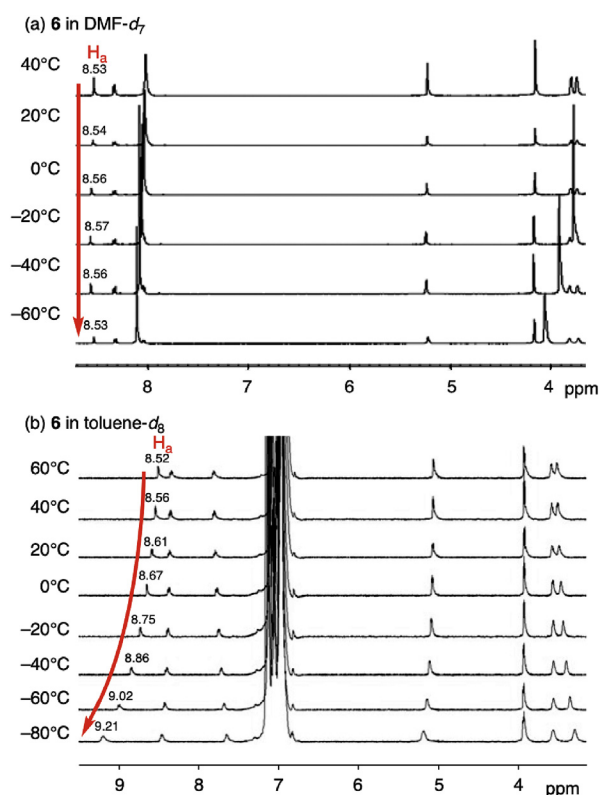


Fig. 4. Variable-temperature ^1H NMR (500 MHz) spectra of **6** in (a) $\text{DMF-}d_7$ and (b) $\text{toluene-}d_8$.

Similar changes in the chemical shift of the resonance for H_a (8.45 ppm at 40°C , 8.61 ppm at -80°C) were observed in a variable-temperature ^1H NMR spectroscopic study of **7** in $\text{toluene-}d_8$. The combined results arising from the variable-temperature fluorescence and ^1H NMR spectroscopic studies suggest that the resonance of H_a of excimer-emitting *syn* form appears at upfield, and that of monomer-emitting *anti* form appears at downfield.

Because pyrenophanes **6** and **7** possess respective 30 and 36

membered crown ether ring systems, it is expected that they would form host-guest complexes with metal ions perhaps in a size selective manner [48–54]. In order to explore this proposal, fluorescence changes were monitored upon addition of perchlorate salts of various metal ions to 1:1 v/v $\text{CH}_3\text{CN}:\text{CH}_2\text{Cl}_2$ solutions of **6** and **7** (Fig. 5a–f). In the case of **6**, addition of metal salts caused a decrease in the intensity of the intramolecular excimer emission band and a simultaneous increase in the intensity of monomer emission along with the existence of isoemissive points. The degree of the change decreased in the order of $\text{Ba}^{2+} > \text{Na}^+ > \text{Li}^+$. The change from intramolecular excimer to monomer emission of pyrenophane **7**, which has a larger ring size, was large when Ba^{2+} cation was present, whereas when Na^+ and Li^+ were present the intensity of intramolecular excimer emission decreased to a lesser extent and monomer emission was unaltered. Analysis of Job's plots [55–57], constructed using the absorption and fluorescence spectroscopic changes, indicated that **6** and **7** form 1:1 complexes as the major species with all of these metal cations (Fig. 5g and h). Inspection of complexation constants K [58] obtained from analysis of the fluorescence changes showed that K values for complexation of metal ions to **6** and **7** decrease in the order of $\text{Ba}^{2+} > \text{Na}^+ > \text{Li}^+$ and that **7** binds Ba^{2+} more strongly than does **6** (Table 1).

Information about structural changes occurring in association with interactions between the pyrenophanes and metal cations came from ^1H NMR analysis of CDCl_3 solutions of **6** and **7** before and after addition of metal perchlorates (Fig. 6). Addition of $\text{Ba}(\text{ClO}_4)_2$ to a CDCl_3 solution of **6** promoted a downfield shift of the resonance for H_a from 8.39 to 8.93 ppm, while addition of NaClO_4 resulted in a slight upfield shift from 8.39 to 8.33 ppm. Similarly, addition of

Table 1

Ionic radii and complexation constants for metal ions.

metal ion	ionic radius (pm) ^a	K (M^{-1}) ^b	
		6	7
Ba^{2+}	135	775 ± 15	9060 ± 290
Na^+	95	286 ± 14	272 ± 13
Li^+	60	162 ± 7	166 ± 11

^a Data from Ref. [59].

^b Complexation constants calculated by using TitrationFit 2014-0630 based on fluorescence changes.

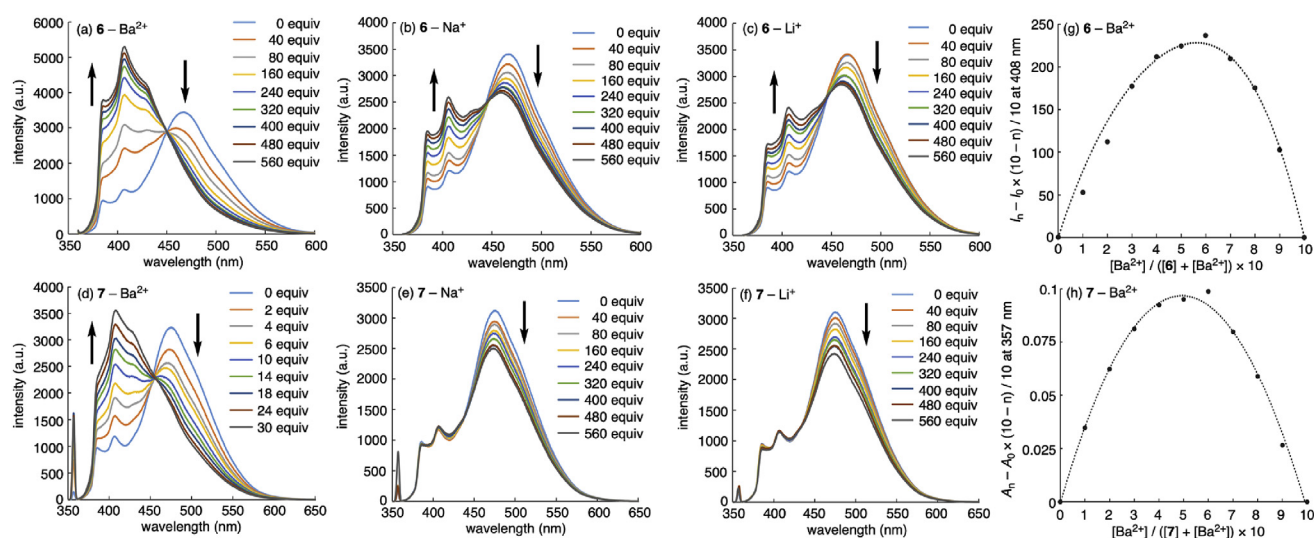


Fig. 5. Fluorescence spectra of (a)–(c) **6**, $\lambda_{\text{ex}} = 358$ nm, and (d)–(f) **7**, $\lambda_{\text{ex}} = 357$ nm, upon addition of (a)(d) $\text{Ba}(\text{ClO}_4)_2$, (b)(e) NaClO_4 , and (c)(f) LiClO_4 , in 1:1 $\text{CH}_3\text{CN}:\text{CH}_2\text{Cl}_2$, [**6** or **7**] = 1.0×10^{-5} M, r.t. (g) Job's plot for complexation of **6** with Ba^{2+} obtained from change of fluorescence intensity at 408 nm, [**6**] + [Ba^{2+}] = 1.0×10^{-5} M, r.t., $\lambda_{\text{ex}} = 358$ nm. (h) Job's plot for complexation of **7** with Ba^{2+} obtained from change of absorbance at 357 nm, [**7**] + [Ba^{2+}] = 1.0×10^{-5} M, r.t.

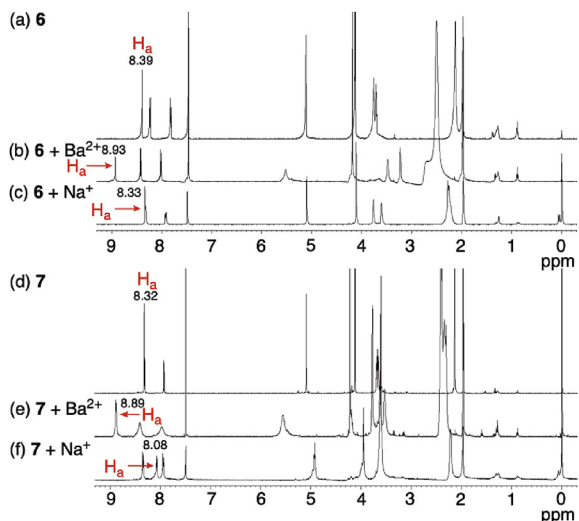


Fig. 6. ^1H NMR (500 MHz, CDCl_3) spectra of (a) **6**, (b) **6** + excess $\text{Ba}(\text{ClO}_4)_2$, (c) **6** + excess NaClO_4 , (d) **7**, (e) **7** + excess $\text{Ba}(\text{ClO}_4)_2$, and (f) **7** + excess NaClO_4 , r.t.

$\text{Ba}(\text{ClO}_4)_2$ to a CDCl_3 solution of **7** caused a downfield shift of H_a from 8.32 to 8.89 ppm, while addition of NaClO_4 induced an upfield shift from 8.32 to 8.08 ppm. Combined inspection of increase of monomer emission and the downfield shift upon addition of $\text{Ba}(\text{ClO}_4)_2$ showed again that resonance of H_a of *anti* conformer appears more downfield than that of *syn* conformer.

Optimized structures of *syn* and *anti* conformers of **6** and of the transition state (TS) in interconversion of the conformers were estimated using DFT calculations with a B3LYP/6-311G basis set (Fig. 7). The results show that *anti*-**6** is 26.2 kJ/mol more stable than *syn*-**6**. The inner protons H_a in *syn*-**6** (marked in Fig. 7) were upfield shifted as a consequence of ring current effect of the opposing pyrene ring. In contrast, H_a of *anti*-**6** did not experience a ring current effect. Because the distance between H_a and the other pyrene ring in *syn* form is larger in **7** than that in **6**, the ring current effect on the chemical shift of H_a in **7** is lower. Dipole moments of *syn*-**6** and *anti*-**6** were determined to be 5.8 and 0.015 D, respectively. This finding is reasonable when consideration is given to the

fact that the dipole moment contributions from the pyrene rings in the *syn* form are additive, whereas in the *anti* conformer those from the pyrene rings are subtractive. Consequently, polar solvents stabilize the ground state (S_0) of *syn*-**6**. Also, the excited state (S_1) of the *syn* conformer can form an intramolecular excimer, which relative to that of the *anti*-conformer, is stabilized by polar solvents such as DMF. Finally, the observed increase in the ratio of intramolecular excimer to monomer emission at higher temperatures in toluene, might also be related to an entropy increase arising from desolvation, a decrease in solvent viscosity [60], fluorescence lifetime [61,62] and an increase in molecular motion. Similar temperature dependency is also found in pyrene (**8**) [2] and 1,3-di(1-pyrenyl)propane [63,64].

(1,8)Pyrenophanes **6** and **7** containing crown ether moieties exist as equilibrium mixtures of *syn* and *anti* conformers (Scheme 3). Addition of metal cations to solutions of **6** and **7** leads to host-guest complex formation and fluorescence and ^1H NMR spectral changes. Inspection of the fluorescence results suggest that structures of the formed complexes differ depending on the sizes of crown ether ring systems and metal cations. The findings indicate that **6** forms $\text{M}^{\text{n}+}$ @*anti* type complexes preferentially with all three metal cations while **7** forms a $\text{M}^{\text{n}+}$ @*anti* type complex with Ba^{2+} and $\text{M}^{\text{n}+}$ @*syn* type complexes with Na^+ and Li^+ [65]. The spectral changes in fluorescence upon addition of Na^+ or Li^+ to solutions of **7** may indicate that the fluorescence intensities of the complexes are smaller than that of the uncomplexed substrate.

3. Conclusion

In the study described above, we prepared seven novel ether-linked (1,8)pyrenophanes and probed their fluorescence and ^1H NMR in order to gain information about their conformational characteristics and metal cation binding properties. In contrast to the mono- and di-ether linked pyrenophanes **1–5** that displayed only monomer-type fluorescence, the oligo-ether tethered substances **6** and **7** displayed both monomer and intramolecular excimer emissions. We observed that solvent, temperature and metal cation binding change the ratios of the intensities of the monomer- and intramolecular excimer-emission in a manner that is consistent with changes in equilibria between the *syn* and *anti* conformers of these substances in the ground, singlet excited and

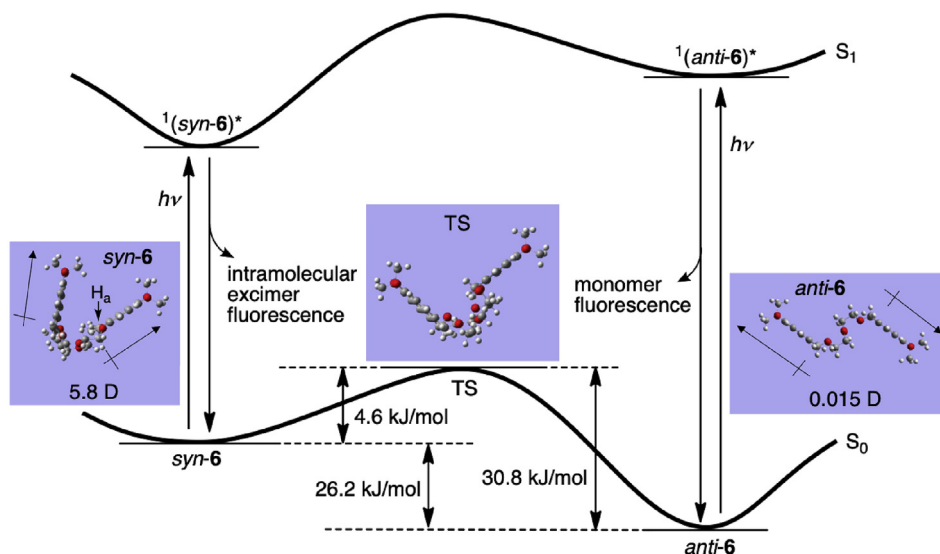
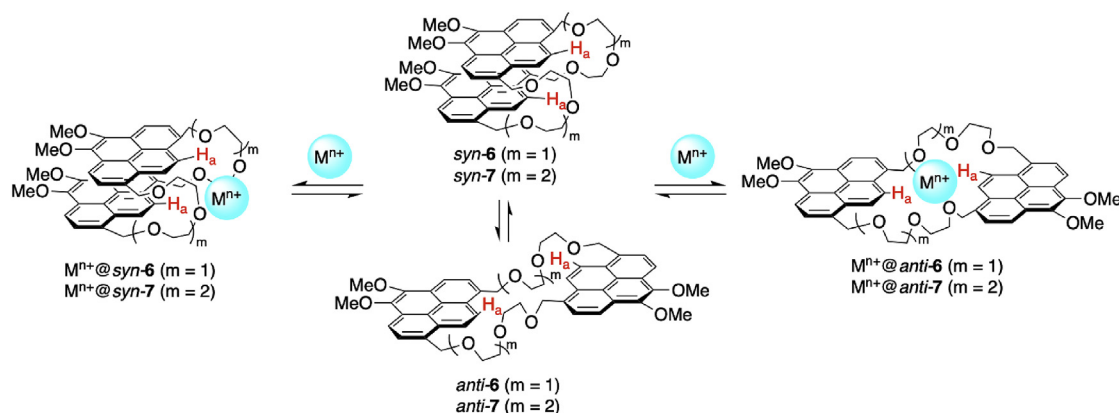


Fig. 7. Energy profiles in interconversion of *anti*-**6** and *syn*-**6** in the ground (S_0) and singlet excited (S_1) states, calculated by using DFT and a B3LYP/6-311G basis set.



Scheme 3. Equilibria between *anti*-6,7 and *syn*-6,7 and their metal complexes.

metal cation complexed states. We anticipate that the emission switching pyrenophanes **6** and **7** will be models for the design of new fluorescence sensors for metal cations.

4. Experimental section

4.1. Materials and equipments

Et₂O and THF were distilled from CaH₂ and then from Na/Ph₂C=O. CH₂Cl₂, CHCl₃, toluene, EtOH, and CH₃CN were distilled from CaH₂. DMF was distilled without drying agent. Spectral grade of CHCl₃, CH₂Cl₂, and DMF were purchased and used for spectroscopic studies without further purification. Most other chemical substances were used after purification by distillation or recrystallization. ¹H and ¹³C NMR spectra were recorded using a JEOL JMN LA-400 (400 MHz and 100 MHz, respectively) or a JEOL ECA-500 (500 MHz and 125 MHz, respectively) spectrometer with Me₄Si as an internal standard. IR spectra were determined using a Shimadzu FTIR-8300 spectrometer. Low- and high-resolution mass spectra were taken on a JEOL JMS-AM50 and a JEOL JMS-SM102A instrument, respectively. UV–vis spectra were recorded using a Hitachi U-2900 spectrophotometer. Fluorescence spectra were recorded using a Jasco FP-8500 spectrophotometer. The fluorescence lifetimes of **1** were measured with a picosecond light pulser (Hamamatsu Photonics C4725, 408 nm, 59 ps FWHM) and a streak-scope (Hamamatsu Photonics C4334-02). HPLC separations were performed on a recycling preparative HPLC instrument (Japan Analytical Industry Co. Ltd., LC-908 equipped with a JAIGEL-H (GPC) column). Column chromatography was conducted by using Kanto-Chemical Co. Ltd., silica gel 60 N (spherical, neutral, 0.04–0.05 mm). Thin-layer chromatography was performed with Merck Kiesel gel 60 F₂₅₄ plates, and spots were detected by using UV light and a phosphomolybdic acid ethanol solution with heating. Theoretical calculations were performed by using B3LYP/6-311G basis set in a Gaussian 09 software package. Complexation constants were calculated by using TitrationFit 2014-0630 based on changes of UV absorption and fluorescence spectra.

4.2. Preparation of 1,8-bis(hydroxymethyl)-4,5-dimethoxyppyrene (**13**)

To a stirred CH₂Cl₂ (90 mL) and THF (90 mL) solution of pyrene (**8**, 6.068 g, 30 mmol) were added NaIO₄ (21.4 g, 100 mmol), H₂O (120 mL), and RuCl₃·nH₂O (0.1 g, 0.4 mmol). The mixture was stirred at room temperature for 24 h and filtered through silica gel using CH₂Cl₂ (200 mL). The filtrate was divided into organic and

aqueous layers, and the aqueous layer was washed with CH₂Cl₂ (50 mL × 3). The combined organic layers were washed with saturated NaCl aqueous solution, dried over Na₂SO₄, filtered, and concentrated in vacuo, giving a residue that was subjected to silica gel column chromatography ($\phi = 5$ cm, $l = 15$ cm, eluent: CH₂Cl₂, $R_f = 0.3$) to give pyrene-4,5-dione (**9**, reddish orange solid, 2.99 g, 45% yield). Lit [38,39].

To a stirred H₂O (50 mL) and THF (50 mL) solution of pyrene-4,5-dione (**9**, 1.758 g, 7.6 mmol) were added *n*-Bu₄NBr (0.79 g, 2.45 mmol) and Na₂S₂O₄ (4.27 g, 24.5 mmol), and the resulting solution was stirred at room temperature for 5 min. To the solution were added NaOH aqueous solution (2.5 M, 40 mL) and Me₂SO₄ (5.17 g, 41 mmol), and the mixture was stirred at room temperature for 12 h and extracted with Et₂O (50 mL). The aqueous layer was washed with Et₂O (30 mL). The combined organic layers were washed with H₂O (50 mL) and then with saturated NaCl aqueous solution (50 mL), dried over Na₂SO₄, filtered, and concentrated in vacuo, giving a residue that was subjected to silica gel column chromatography ($\phi = 5$ cm, $l = 15$ cm, eluent: CHCl₃, $R_f = 0.8$) to give 4,5-dimethoxyppyrene (**10**, ochre solid, 1.81 g, 92% yield). Lit [40].

To an argon-purged, stirred CH₂Cl₂ (20 mL) solution of 4,5-dimethoxyppyrene (**10**, 1.004 g, 3.8 mmol) Br₂ was added dropwise (0.44 mL, 8.4 mmol), and the resulting solution was stirred at room temperature for 5 min. NaOH aqueous solution (20%, 20 mL) was added and the formed precipitate was collected by filtration and characterized as the product **11**. The filtrate was extracted with CH₂Cl₂ (50 mL). The aqueous layer was washed with CH₂Cl₂ (30 mL × 2). The combined organic layers were washed with NaCl aqueous solution (50 mL), dried over Na₂SO₄, filtered, and concentrated in vacuo, giving a residue that was subjected to silica gel column chromatography ($\phi = 5$ cm, $l = 15$ cm, eluent: CH₂Cl₂, $R_f = 0.95$) to give 1,8-dibromo-4,5-dimethoxyppyrene (**11**, white solid, 1.41 g, 87% yield). Lit [40].

To an argon-purged, stirred THF (120 mL) solution of 1,8-dibromo-4,5-dimethoxyppyrene (**11**, 1.890 g, 4.5 mmol) was added slowly *tert*-BuLi (1.6 M in pentane, 16 mL, 25 mmol) at -78 °C, and the resulting solution was stirred at -78 °C for 1 h. To the solution was added slowly DMF (0.733 g, 10 mmol), and the resulting solution was stirred at room temperature for 1 h. H₂O (150 mL) was slowly added and the resulting solution was extracted with CH₂Cl₂ (50 mL). The aqueous layer was washed with CH₂Cl₂ (50 mL × 3). The combined organic layers were washed with HCl aqueous solution (1 N, 50 mL) and then with saturated NaCl aqueous solution (50 mL), dried over Na₂SO₄, filtered, and concentrated in vacuo to give a solid that was washed with acetone and collected by

filtration to give 1,8-diformyl-4,5-dimethoxyppyrene (**12**, 1.10 g, 75% yield). Data for **12**: dark yellow solid; mp 219–222 °C; ^1H NMR (400 MHz, CDCl_3) δ 4.27 (s, 6H), 8.54 (d, $J = 8.0$ Hz, 2H), 8.71 (d, $J = 8.0$ Hz, 2H) 9.56 (s, 2H), 10.82 (s, 2H) ppm; ^{13}C NMR (100 MHz, CDCl_3) δ 61.42, 120.66, 122.36, 126.09, 128.00, 129.92, 131.88, 132.95, 146.55, 192.71 ppm; IR (KBr) 1026, 1203, 1492, 1612, 1685, 2742 cm^{-1} ; MS (EI) m/z (relative intensity, %) = 198 (1), 231 (13), 259 (10), 275 (7), 303 (27), 318 (100, M^+); HRMS (EI) calcd for $\text{C}_{20}\text{H}_{14}\text{O}_4$: 318.0892, found: 318.0897.

To a stirred THF (60 mL) solution of 1,8-diformyl-4,5-dimethoxyppyrene (**12**, 0.79 g, 2.5 mmol) were added NaBH_4 (0.39 g, 10.2 mmol) and EtOH (6 mL) at 0 °C, and the mixture was stirred at 0 °C for 1 h. HCl (1 N, 50 mL) was slowly added. The solution was extracted with Et_2O (40 mL) and the aqueous layer was washed with Et_2O (30 mL). The combined organic layers were washed with saturated NaCl aqueous solution (40 mL), dried over Na_2SO_4 , filtered, and concentrated in vacuo to give a solid that was washed with CHCl_3 and collected by filtration to give 1,8-bis(hydroxymethyl)-4,5-dimethoxyppyrene (**13**, 0.58 g, 72% yield). Data for **13**: yellow solid; mp 160–164 °C; ^1H NMR (400 MHz, CDCl_3) δ 1.58 (brs, 2H), 4.21 (s, 6H), 5.43 (s, 4H), 8.10 (d, $J = 8.0$ Hz, 2H), 8.47 (s, 2H), 8.48 (d, $J = 8.0$ Hz, 2H) ppm; ^{13}C NMR (100 MHz, CDCl_3) δ 61.18, 63.84, 119.42, 123.42, 123.54, 126.37, 128.57, 128.66, 133.61, 144.52 ppm; IR (KBr) 961, 1103, 1196, 1227, 1304, 1396, 1612, 2847, 3344 cm^{-1} ; MS (EI) m/z (relative intensity, %) = 44 (7), 77 (13), 105 (6), 149 (12), 218 (10), 231 (17), 307 (35), 322 (100, M^+); HRMS (EI) calcd for $\text{C}_{20}\text{H}_{18}\text{O}_4$: 322.1205, found: 322.1209.

4.3. Preparation of 1,8-bis(bromomethyl)-4,5-dimethoxyppyrene (**14**)

To an argon-purged, stirred Et_2O (50 mL) solution of 1,8-bis(hydroxymethyl)-4,5-dimethoxyppyrene (**13**, 0.805 g, 2.5 mmol) was added a CHCl_3 (10 mL) solution of PBr_3 (2.3 g, 8.4 mmol). The resulting solution was stirred at room temperature for 24 h. Saturated NH_4Cl aqueous solution (30 mL) was added, and the solution was stirred at room temperature for 10 min. H_2O (20 mL) was added. The solution was extracted with CH_2Cl_2 (30 mL) and the aqueous layer was washed with CH_2Cl_2 (30 mL \times 3). The combined organic layers were washed with saturated NaCl aqueous solution (30 mL), dried over Na_2SO_4 , filtered, and concentrated in vacuo to give 1,8-bis(bromomethyl)-4,5-dimethoxyppyrene (**14**, 0.764 g, 68% yield). Data for **14**: yellow solid; mp 204–207 °C (dec); ^1H NMR (400 MHz, CDCl_3) δ 4.19 (s, 6H), 5.25 (s, 4H), 8.05 (d, $J = 8.0$ Hz, 2H), 8.46 (d, $J = 8.0$ Hz, 2H), 8.51 (s, 2H) ppm; ^{13}C NMR (100 MHz, CDCl_3) δ 31.81, 61.21, 119.83, 123.37, 123.59, 128.19, 128.70, 129.35, 130.78, 144.93 ppm; IR (KBr) 640, 1230, 1500, 1604, 2842, 2935 cm^{-1} ; MS (EI) m/z (relative intensity, %) = 226 (68), 288 (100), 367 (68), 448 (13, M^+); HRMS (EI) calcd for $\text{C}_{20}\text{H}_{16}\text{Br}_2\text{O}_2$: 447.9497, found: 447.9498.

4.4. Preparation of 1,8-bis(iodomethyl)-4,5-dimethoxyppyrene (**15**)

To an argon-purged, stirred CH_3CN (10 mL) solution of 1,8-bis(hydroxymethyl)-4,5-dimethoxyppyrene (**13**, 0.161 g, 1 mmol) were added NaI (0.45 g, 3 mmol) and Me_3SiCl (0.32 g, 3 mmol), and the resulting solution was stirred at room temperature for 30 min [66]. H_2O (20 mL) was added. The formed bright yellow solid was collected by filtration with CH_3CN to give 1,8-bis(iodomethyl)-4,5-dimethoxyppyrene (**15**, 0.178 g, 65% yield). This product is unstable under air at room temperature and undergoes decomposition to produce a black residue within 3 days. Data for **15**: mp 147–152 °C (dec); ^1H NMR (400 MHz, CDCl_3) δ 4.18 (s, 6H), 5.22 (s, 4H), 8.06 (d, $J = 8.0$ Hz, 2H), 8.42 (d, $J = 8.0$ Hz, 2H), 8.51 (s, 2H) ppm; IR (KBr) 1226, 1497, 1604, 2935 cm^{-1} ; MS (EI) m/z (relative intensity, %) = 83

(100), 288 (32), 415 (24), 542 (2, M^+); HRMS (EI) calcd for $\text{C}_{20}\text{H}_{16}\text{I}_2\text{O}_2$: 541.9240, found: 541.9296.

4.5. Preparation of pyrenophane **1**

A mixture of 1,8-bis(hydroxymethyl)-4,5-dimethoxyppyrene (**13**, 0.16 g, 0.5 mmol) and NaH (60% in mineral oil, 0.8 g, 20 mmol) in THF (120 mL) was stirred at room temperature for 1 h under an argon atmosphere. To the solution was added dropwise a THF (45 mL) solution of 1,8-bis(bromomethyl)-4,5-dimethoxyppyrene (**14**, 0.26 g, 0.5 mmol) over a 2 h period, and the resulting solution was stirred at reflux for 3 days. Ice water (50 mL) was slowly added. The solution was extracted with CHCl_3 (50 mL) and the aqueous layer was washed with CHCl_3 (50 mL \times 3). The combined organic layers were washed with saturated NaCl aqueous solution (50 mL), dried over Na_2SO_4 , filtered, and concentrated in vacuo, giving a residue that was subjected to silica gel column chromatography ($\phi = 3$ cm, $l = 15$ cm, eluent: CHCl_3 :EtOH = 30:1, $R_f = 0.4$) followed by recycling preparative HPLC (GPC, eluent: CHCl_3) to give 7,8,20,21-tetramethoxy-2,15-dioxo[3.3](1,8)pyrenophane (**1**, 0.010 g, 7% yield). Data for **1**: pale yellow solid; mp 234–236 °C; ^1H NMR (400 MHz, CDCl_3) δ 4.22 (s, 12H), 5.16 (s, 8H), 7.48 (s, 4H), 8.02 (d, $J = 8.0$ Hz, 4H), 8.40 (d, $J = 8.0$ Hz, 4H) ppm; ^{13}C NMR (100 MHz, CDCl_3) δ 61.22, 70.53, 118.53, 123.35, 124.99, 128.56, 129.70, 131.74, 144.64, 169.74 ppm; IR (KBr) 1230, 1500, 1604, 2854, 2927 cm^{-1} ; MS (EI) m/z (relative intensity, %) = 260 (6), 288 (8), 320 (4), 608 (100, M^+); HRMS (EI) calcd for $\text{C}_{40}\text{H}_{32}\text{O}_6$: 608.2199, found: 608.2219.

4.6. Preparation of pyrenophane **2**

A mixture of ethylene glycol (0.068 g, 1.1 mmol) and NaH (60% in mineral oil, 0.8 g, 20 mmol) in THF (100 mL) was stirred at reflux for 1 h under an argon atmosphere. To the solution was added dropwise a THF (40 mL) solution of 1,8-bis(bromomethyl)-4,5-dimethoxyppyrene (**14**, 0.448 g, 1.0 mmol) over a 1 h period, and the resulting solution was stirred at reflux for 3 days. Ice water (30 mL) was slowly added. The solution was extracted with CH_2Cl_2 (30 mL) and the aqueous layer was washed with CH_2Cl_2 (30 mL \times 3). The combined organic layers were washed with saturated NaCl aqueous solution (30 mL), dried over Na_2SO_4 , filtered, and concentrated in vacuo, giving a residue that was subjected to silica gel column chromatography ($\phi = 3$ cm, $l = 15$ cm, eluent: CH_2Cl_2 :EtOH = 30:1, $R_f = 0.3$) followed by recycling preparative HPLC (GPC, eluent: CHCl_3) to give 10,11,26,27-tetramethoxy-2,5,18,21-tetraoxa[6.6](1,8)pyrenophane (**2**, 0.049 g, 14% yield). Data for **2**: ochre solid; mp 232–234 °C; ^1H NMR (500 MHz, CDCl_3) δ 3.96 (s, 8H), 4.17 (s, 12H), 5.22 (s, 8H), 7.97 (d, $J = 7.5$ Hz, 4H), 8.40 (d, $J = 8.0$ Hz, 4H), 8.79 (s, 4H) ppm; ^{13}C NMR (100 MHz, CDCl_3) δ 61.13, 70.92, 72.65, 118.88, 118.91, 124.40, 127.64, 128.61, 129.51, 129.53, 131.18, 131.21, 144.44 ppm; IR (KBr) 1226, 1465, 1608, 2881, 2950 cm^{-1} ; MS (FAB+) m/z (relative intensity, %) = 289(28), 349(11), 409(3), 697(48); HRMS (FAB+) calcd for $\text{C}_{44}\text{H}_{41}\text{O}_8$: 697.2801, found: 697.2792.

4.7. Preparation of pyrenophane **3**

A mixture of 1,3-propanediol (0.084 g, 1.1 mmol) and NaH (60% in mineral oil, 0.8 g, 20 mmol) in THF (100 mL) was stirred at reflux for 1 h under an argon atmosphere. To the solution was added dropwise a THF (40 mL) solution of 1,8-bis(bromomethyl)-4,5-dimethoxyppyrene (**14**, 0.448 g, 1.0 mmol) over a 1 h period, and the resulting solution was stirred at reflux for 3 days. Ice water (30 mL) was slowly added. The solution was extracted with CH_2Cl_2 (30 mL) and the aqueous layer was washed with CH_2Cl_2

(30 mL \times 3). The combined organic layers were washed with saturated NaCl aqueous solution (30 mL), dried over Na₂SO₄, filtered, and concentrated in vacuo, giving a residue that was subjected to silica gel column chromatography (ϕ = 3 cm, l = 15 cm, eluent: CH₂Cl₂:EtOH = 30:1, R_f = 0.3) followed by recycling preparative HPLC (GPC, eluent: CHCl₃) to give 11,12,28,29-tetramethoxy-2,6,19,23-tetraoxa[7.7](1,8)pyrenophane (**3**, 0.064 g, 18% yield). Data for **3**: ocher solid; mp 181–182 °C; ¹H NMR (500 MHz, CDCl₃) δ 1.99 (quint, J = 5.3 Hz, 4H), 3.76 (t, J = 5.5 Hz, 8H) 4.20 (s, 12H) 5.02 (s, 8H), 7.56 (d, J = 8.0 Hz, 4H), 8.08 (d, J = 8.0 Hz, 4H), 8.11 (s, 4H) ppm; ¹³C NMR (100 MHz, CDCl₃) δ 30.08, 60.94, 65.38, 71.15, 118.26, 122.73, 125.22, 127.79, 130.89, 144.04 ppm; IR (KBr) 1137, 1226, 2850, 2920 cm⁻¹; MS (FAB+) m/z (relative intensity, %) = 226 (5), 288 (42), 724 (60, M⁺); HRMS (FAB+) calcd for C₄₆H₄₄O₈: 724.3038, found: 724.3024.

4.8. Preparation of pyrenophane **4**

A mixture of 1,4-butanediol (0.099 g, 1.1 mmol) and NaH (60% in mineral oil, 0.8 g, 20 mmol) in THF (120 mL) was stirred at reflux for 1 h under an argon atmosphere. To the solution was added dropwise a THF (50 mL) solution of 1,8-bis(iodomethyl)-4,5-dimethoxy-pyrene (**15**, 0.542 g, 1.0 mmol) over a 1 h period, and the resulting solution was stirred at reflux for 3 days. Ice water (30 mL) was slowly added. The solution was extracted with CHCl₃ (30 mL) and the aqueous layer was washed with CHCl₃ (30 mL \times 3). The combined organic layers were washed with saturated NaCl aqueous solution (30 mL), dried over Na₂SO₄, filtered, and concentrated in vacuo, giving a residue that was subjected to silica gel column chromatography (ϕ = 3 cm, l = 15 cm, eluent: CH₂Cl₂:EtOH = 30:1, R_f = 0.35–0.45) followed by recycling preparative HPLC (GPC, eluent: CHCl₃) to give 12,13,30,31-tetramethoxy-2,7,20,25-tetraoxa[8.8](1,8)pyrenophane (**4**, 0.023 g, 6% yield). Data for **4**: ocher solid; mp 169–171 °C; ¹H NMR (500 MHz, CDCl₃) δ 1.70–1.75 (m, 8H), 3.55–3.60 (m, 8H), 4.18 (s, 12H), 5.08 (s, 8H), 7.95 (d, J = 8.0 Hz, 4H), 8.40 (d, J = 8.0 Hz, 4H), 8.50 (s, 4H) ppm; ¹³C NMR (100 MHz, CDCl₃) δ 22.64, 29.32, 61.11, 69.88, 71.66, 118.77, 123.31, 123.91, 127.30, 128.51, 129.27, 131.33, 144.38 ppm; IR (KBr) 1099, 1226, 2855, 2924 cm⁻¹; MS (FAB+) m/z (relative intensity, %) = 226 (2), 288 (28), 752 (12, M⁺); HRMS (FAB+) calcd for C₄₈H₄₈O₈: 752.3349, found: 752.3335.

4.9. Preparation of pyrenophane **5**

A mixture of 1,5-pentanediol (0.115 g, 1.1 mmol) and NaH (60% in mineral oil, 0.8 g, 20 mmol) in THF (120 mL) was stirred at reflux for 1 h under an argon atmosphere. To the solution was added dropwise a THF (30 mL) solution of 1,8-bis(bromomethyl)-4,5-dimethoxy-pyrene (**14**, 0.448 g, 1.0 mmol) over a 1 h period, and the resulting solution was stirred at reflux for 3 days. Ice water (30 mL) was slowly added. The solution was extracted with CHCl₃ (30 mL) and the aqueous layer was washed with CHCl₃ (30 mL \times 3). The combined organic layers were washed with saturated NaCl aqueous solution (30 mL), dried over Na₂SO₄, filtered, and concentrated in vacuo, giving a residue that was subjected to silica gel column chromatography (ϕ = 3 cm, l = 10 cm, eluent: CH₂Cl₂:EtOH = 30:1, R_f = 0.35–0.45) followed by recycling preparative HPLC (GPC, eluent: CHCl₃) to give 13,14,32,33-tetramethoxy-2,8,21,27-tetraoxa[9.9](1,8)pyrenophane (**5**, 0.035 g, 10% yield). Data for **5**: ocher solid; mp 166–167 °C; ¹H NMR (500 MHz, CDCl₃) δ 1.52–1.66 (m, 12H), 3.46–3.52 (m, 8H), 4.16 (s, 12H), 5.07 (s, 8H), 7.93 (d, J = 8.0 Hz, 4H), 8.36 (d, J = 8.0 Hz, 4H) 8.40 (s, 4H) ppm; ¹³C NMR (100 MHz, CDCl₃) δ 22.64, 29.32, 61.11, 69.88, 71.66, 118.77, 123.31, 123.91, 127.30, 128.51, 129.27, 131.33, 144.38 ppm; IR (KBr) 1191, 1227, 2858, 2932 cm⁻¹; MS (EI) m/z (relative intensity,

%) = 226 (2), 288 (9), 780 (15, M⁺); HRMS (FAB+) calcd for C₅₀H₅₂O₈: 780.3662, found: 780.3659.

4.10. Preparation of pyrenophane **6**

A mixture of diethylene glycol (0.106 g, 1.0 mmol) and NaH (60% in mineral oil, 0.8 g, 20 mmol) in THF (100 mL) was stirred at room temperature for 1 h under an argon atmosphere. To the solution was added dropwise a THF (45 mL) solution of 1,8-bis(bromomethyl)-4,5-dimethoxy-pyrene (**14**, 0.448 g, 1.0 mmol) over a 1 h period, and the resulting solution was stirred at reflux for 3 days. Ice water (30 mL) was slowly added. The solution was extracted with CHCl₃ (30 mL) and the aqueous layer was washed with CHCl₃ (30 mL \times 3). The combined organic layers were washed with saturated NaCl aqueous solution (30 mL), dried over Na₂SO₄, filtered, and concentrated in vacuo, giving a residue that was subjected to silica gel column chromatography (ϕ = 3 cm, l = 15 cm, eluent: CHCl₃:EtOH = 30:1, R_f = 0.35) followed by recycling preparative HPLC (GPC, eluent: CHCl₃) to give 13,14,32,33-tetramethoxy-2,5,8,21,24,27-hexaoxa[9.9](1,8)pyrenophane (**6**, 0.020 g, 18% yield). Data for **6**: orange solid; mp 191–193 °C; ¹H NMR (400 MHz, CDCl₃) δ 3.69–3.76 (m, 16H), 4.15 (s, 12H), 5.16 (s, 8H), 7.86 (d, J = 8.0 Hz, 4H), 8.29 (d, J = 8.0 Hz, 4H), 8.45 (s, 4H) ppm; ¹³C NMR (100 MHz, CDCl₃) δ 61.09, 69.44, 70.92, 71.95, 118.70, 123.19, 123.97, 127.32, 128.44, 129.24, 131.01, 144.36 ppm; IR (KBr) 829, 1137, 1504, 1612, 2862 cm⁻¹; MS (FAB+) m/z (relative intensity, %) = 226 (1), 288 (23), 784 (10, M⁺); HRMS (FAB+) calcd for C₄₈H₄₉O₁₀: 785.3247, found: 785.3335.

4.11. Preparation of pyrenophane **7**

A mixture of triethylene glycol (0.165 g, 1.1 mmol) and NaH (60% in mineral oil, 0.8 g, 20 mmol) in THF (120 mL) was stirred at reflux for 1 h under an argon atmosphere. To the solution was added dropwise a THF (35 mL) solution of 1,8-bis(bromomethyl)-4,5-dimethoxy-pyrene (**14**, 0.448 g, 1.0 mmol) over a 1 h period, and the resulting solution was stirred at reflux for 3 days. Ice water (30 mL) was slowly added. The solution was extracted with CHCl₃ (30 mL) and the aqueous layer was washed with CHCl₃ (30 mL \times 3). The combined organic layers were washed with saturated NaCl aqueous solution (30 mL), dried over Na₂SO₄, filtered, and concentrated in vacuo, giving a residue that was subjected to silica gel column chromatography (ϕ = 3 cm, l = 10 cm, eluent: CH₂Cl₂:EtOH = 15:1, R_f = 0.45–0.55) followed by recycling preparative HPLC (GPC, eluent: CHCl₃) to give 16,17,38,39-tetramethoxy-2,5,8,11,24,27,30,33-octaoxa[12.12](1,8)pyrenophane (**7**, 0.047 g, 12% yield) and 16,17-dimethoxy-2,5,8,11-tetraoxa[12](1,8)pyrenophane (**16**, 0.068 g, 16% yield). Data for **7**: yellow solid; mp 157–160 °C; ¹H NMR (500 MHz, CDCl₃) δ 3.62–3.68 (m, 24H), 4.16 (s, 12H), 5.16 (s, 8H), 7.93 (d, J = 8.0 Hz, 4H), 8.36 (d, J = 8.0 Hz, 4H), 8.41 (s, 4H) ppm; ¹³C NMR (100 MHz, CDCl₃) δ 61.09, 69.56, 70.69, 70.73, 71.98, 118.79, 123.17, 123.94, 127.52, 128.51, 129.28, 130.97, 144.37 ppm; IR (KBr) 1134, 1226, 2858 cm⁻¹; MS (FAB+) m/z (relative intensity, %) = 226 (2), 288 (8), 872 (6, M⁺). HRMS (FAB+) calcd for C₅₂H₅₆O₁₂: 872.3772, found: 872.3777. Data for **16**: ocher solid; mp 143–145 °C; ¹H NMR (400 MHz, CDCl₃) δ 3.50 (s, 4H), 3.58–3.61 (m, 8H), 4.20 (s, 6H), 5.29 (s, 4H), 7.91 (d, J = 7.6 Hz, 2H), 8.38 (d, J = 8.0 Hz, 2H), 8.67 (s, 2H) ppm; ¹³C NMR (100 MHz, CDCl₃) δ 61.15, 69.34, 70.57, 71.02, 72.94, 118.32, 123.23, 125.05, 127.47, 128.84, 129.76, 131.33, 144.53 ppm; IR (KBr) 1099, 1227, 2878, 2947 cm⁻¹; MS (FAB+) m/z (relative intensity, %) = 226 (1), 288 (49), 436 (100, M⁺). HRMS (FAB+) calcd for C₂₆H₂₈O₆: 436.1886, found: 436.1893.

Acknowledgments

This study was financially supported by a Grant-in-Aid for Scientific Research (C) (20550049, 23550047, 26410040, 17K05777) from the Ministry of Education, Culture, Sports, Science and Technology (MEXT) of Japan. H. M. is also grateful for financial support from The Mazda Foundation, The Murata Science Foundation, Izumi Science and Technology Foundation, Shibuya Science Culture and Sports Foundation, A-STEP (Adaptable and Seamless Technology Transfer Program through target-driven R&D, JST, Japan), and Kanazawa University SAKIGAKE Project. We thank Professor Tsuyoshi Asakawa, Associate Professor Akio Ohta, Professor Tadaaki Yamagishi, and Professor Tomoki Ogoshi at Kanazawa University for permission to use UV-vis absorption and fluorescence spectrophotometers. We thank Professor Seiichi Nishizawa at Tohoku University for permission to use fluorescence lifetime measurement system. We are also indebted to Professor Shigehisa Akine at Kanazawa University for donation of the TitrationFit 2014-0630 program.

Appendix A. Supplementary data

Supplementary data to this article can be found online at <https://doi.org/10.1016/j.tet.2019.130512>.

References

- [1] J.B. Birks, *Acta Phys. Pol.* 34 (1968) 603–617.
- [2] Th. Förster, *Angew. Chem. Int. Ed.* 8 (1969) 333–343.
- [3] K. Zachariasse, W. Kühnle, *Z. Phys. Chem.* 101 (1976) S267–S276.
- [4] F.C. De Schryver, P. Collart, J. Vandendriessche, R. Goedeweck, A.M. Swinnen, M. Van der Auweraer, *Acc. Chem. Res.* 20 (1987) 159–166.
- [5] F.M. Winnik, *Chem. Rev.* 93 (1993) 587–614.
- [6] S. Karuppanan, J.-C. Chambron, *Chem. Asian J.* 6 (2011) 964–984.
- [7] M.E. Østergaard, P.J. Hrdlicka, *Chem. Soc. Rev.* 40 (2011) 5771–5788.
- [8] T.M. Figueira-Duarte, K. Müllen, *Chem. Rev.* 111 (2011) 7260–7314.
- [9] G. Bains, A.B. Patel, V. Narayanaswami, *Molecules* 16 (2011) 7909–7935.
- [10] E. Manandhar, K.J. Wallace, *Inorg. Chim. Acta* 381 (2012) 15–43.
- [11] J. Duhamel, *Langmuir* 28 (2012) 6527–6538.
- [12] J.J. Bryant, U.H.F. Bunz, *Chem. Asian J.* 8 (2013) 1354–1367.
- [13] J.M. Casas-Solvas, J.D. Howgego, A.P. Davis, *Org. Biomol. Chem.* 12 (2014) 212–232.
- [14] X. Feng, J.-Y. Hu, C. Redshaw, T. Yamato, *Chem. Eur. J.* 22 (2016) 11898–11916.
- [15] P.G. Ghasemabadi, T. Yao, G. Bodwell, *J. Chem. Soc. Rev.* 44 (2015) 6494–6518.
- [16] T. Umemoto, S. Satani, Y. Sakata, S. Misumi, *Tetrahedron Lett.* 16 (1975) 3159–3162.
- [17] R.H. Mitchell, R.J. Carruthers, J.C.M. Zwinkels, *Tetrahedron Lett.* 17 (1976) 2585–2588.
- [18] H. Irngartinger, R.G.H. Kirrstetter, C. Krieger, H. Rodewald, H.A. Staab, *Tetrahedron Lett.* 18 (1977) 1425–1428.
- [19] K. Ishizu, Y. Sugimoto, T. Umemoto, Y. Sakata, S. Misumi, *Bull. Chem. Soc. Jpn.* 50 (1977) 2801–2802.
- [20] Y. Kai, F. Hama, N. Yasuoka, N. Kasai, *Acta Crystallogr. B* 34 (1978) 1263–1270.
- [21] H.A. Staab, R.G.H. Kirrstetter, *Liebigs Ann. Chem.* (1979) 886–898.
- [22] S. Ishikawa, J. Nakamura, S. Iwata, M. Sumitani, S. Nagakura, Y. Sakata, S. Misumi, *Bull. Chem. Soc. Jpn.* 52 (1979) 1346–1350.
- [23] A. Terahara, H. Ohya-Nishiguchi, N. Hirota, Y. Sakata, S. Misumi, K. Ishizu, *Bull. Chem. Soc. Jpn.* 55 (1982) 3896–3898.
- [24] H.A. Staab, N. Riegler, F. Diederich, C. Krieger, D. Schweitzer, *Chem. Ber.* 117 (1984) 246–259.
- [25] P. Reynders, W. Kühnle, K.A. Zachariasse, *J. Am. Chem. Soc.* 112 (1990) 3929–3939.
- [26] T. Kawashima, T. Otsubo, Y. Sakata, S. Misumi, *Tetrahedron Lett.* 19 (1978) 5115–5118.
- [27] M. Inouye, K. Fujimoto, M. Furusyo, H. Nakazumi, *J. Am. Chem. Soc.* 121 (1999) 1452–1458.
- [28] H. Abe, Y. Mawatari, H. Teraoka, K. Fujimoto, M. Inouye, *J. Org. Chem.* 69 (2004) 495–504.
- [29] H. Hayashi, N. Matsumura, K. Mizuno, *J. Chem. Res.* (2004) 599–601.
- [30] K. Imai, S. Hatano, A. Kimoto, J. Abe, Y. Tamai, N. Nemoto, *Tetrahedron* 66 (2010) 8012–8017.
- [31] Y. Sagara, N. Tamaoki, *RSC Adv.* 7 (2017) 47056–47062.
- [32] T. Umemoto, T. Kawashima, Y. Sakata, S. Misumi, *Chem. Lett.* 4 (1975) 837–840.
- [33] T. Hayashi, N. Mataga, Y. Sakata, S. Misumi, *Chem. Phys. Lett.* 41 (1976) 325–328.
- [34] T. Hayashi, N. Mataga, T. Umemoto, Y. Sakata, S. Misumi, *J. Phys. Chem.* 81 (1977) 424–429.
- [35] T. Yamato, A. Miyazawa, M. Tashiro, *J. Chem. Soc. Perkin Trans. 1* (1993) 3127–3137.
- [36] H. Maeda, M. Hironishi, R. Ishibashi, K. Mizuno, M. Segi, *Photochem. Photobiol. Sci.* 16 (2017) 228–237.
- [37] H. Maeda, K. Nakamura, T. Furuyama, M. Segi, *Photochem. Photobiol. Sci.* (2019), <https://doi.org/10.1039/C9PP00239A> in press.
- [38] J. Hu, D. Zhang, F.W. Harris, *J. Org. Chem.* 70 (2005) 707–708.
- [39] J.C. Walsh, K.-L.M. Williams, D. Lungerich, G.J. Bodwell, *Eur. J. Org. Chem.* (2016) 5933–5936.
- [40] G. Venkataramana, P. Dongare, L.N. Dawe, D.W. Thompson, Y. Zhao, G.J. Bodwell, *Org. Lett.* 13 (2011) 2240–2243.
- [41] A.M. Dmytrejchuk, S.N. Jackson, R. Meudom, J.D. Gorden, B.L. Merner, *J. Org. Chem.* 83 (2018) 10660–10667.
- [42] H. Maeda, K. Hirose, M. Segi, *J. Lumin.* 204 (2018) 269–277.
- [43] I. Yamaguchi, K. Sato, *Bull. Chem. Soc. Jpn.* 86 (2013) 1174–1182.
- [44] F. Lu, N. Kitamura, T. Takaya, K. Iwata, T. Nakanishi, Y. Kurashige, *Phys. Chem. Chem. Phys.* 20 (2018) 3258–3264.
- [45] C. Reichardt, *Chem. Rev.* 94 (1994) 2319–2358.
- [46] N. Sadhukhan, T. Muraoka, D. Abe, Y. Sasanuma, D.R.G. Subekti, K. Kinbara, *Chem. Lett.* 43 (2014) 1055–1057.
- [47] S. Kawasaki, T. Muraoka, H. Obara, T. Ishii, T. Hamada, K. Kinbara, *Chem. Asian J.* 9 (2014) 2778–2788.
- [48] K.E. Krakowiak, J.S. Bradshaw, D.J. Zamecka-Krakowiak, *Chem. Rev.* 89 (1989) 929–972.
- [49] G.W. Gokel (Ed.), *Crown Ethers & Cryptands*, Royal Society of Chemistry, London, 1991.
- [50] R. Cacciapaglia, L. Mandolini, *Chem. Soc. Rev.* 22 (1993) 221–231.
- [51] A.P. de Silva, D.B. Fox, A.J.M. Huxley, T.S. Moody, *Coord. Chem. Rev.* 205 (2000) 41–57.
- [52] S. Fery-Forgues, F. Al-Ali, *J. Photochem. Photobiol. C* 5 (2004) 139–153.
- [53] G.W. Gokel, W.M. Leevy, M.E. Weber, *Chem. Rev.* 104 (2004) 2723–2750.
- [54] J. Li, D. Yim, W.-D. Jang, J. Yoon, *Chem. Soc. Rev.* 46 (2017) 2437–2458.
- [55] J.S. Renny, L.L. Tomasevich, E.H. Tallmadge, D.B. Collum, *Angew. Chem. Int. Ed.* 52 (2013) 11998–12013.
- [56] F. Ulatowski, K. Dabrowa, T. Balakier, J. Jurczak, *J. Org. Chem.* 81 (2016) 1746–1756.
- [57] D.B. Hibbert, P. Thordarson, *Chem. Commun.* 52 (2016) 12792–12805.
- [58] P. Thordarson, *Chem. Soc. Rev.* 40 (2011) 1305–1323.
- [59] L. Pauling (Ed.), *The Nature of the Chemical Bond*, third ed., Cornell University Press, Ithaca, NY, 1960.
- [60] A.L. Macanita, K.A. Zachariasse, *J. Phys. Chem. A* 115 (2011) 3183–3195.
- [61] A. Siemiarzuk, W.R. Ware, *J. Phys. Chem.* 93 (1989) 7609–7618.
- [62] K.A. Zachariasse, W. Kühnle, U. Leinhos, P. Reynders, G. Striker, *J. Phys. Chem.* 95 (1991) 5476–5488.
- [63] M.J. Snare, P.J. Thistlethwaite, K.P. Ghiggino, *J. Am. Chem. Soc.* 105 (1983) 3328–3332.
- [64] D. Declercq, P. Delbeke, F.C. De Schryver, L. Van Meervelt, R.D. Miller, *J. Am. Chem. Soc.* 115 (1993) 5702–5708.
- [65] M. Kida, M. Kubo, T. Ujihira, T. Ebata, M. Abe, Y. Inokuchi, *ChemPhysChem* 19 (2018) 1331–1335.
- [66] G.A. Olah, S.C. Narang, B.G.B. Gupta, R. Malhotra, *J. Org. Chem.* 44 (1979) 1247–1251.